

Space-time visualization of dengue fever outbreaks

[Working chapter]

Eric Delmelle*, Meijuan Jia*, Coline Dony*, Irene Casas[^], Wenwu Tang*

*Center for Applied GIScience and Department of Geography and Earth Sciences
University of North Carolina at Charlotte
eric.delmelle, mjia2, cdony, wenwutang@uncc.edu

[^]Louisiana Tech University
icasas@latech.edu

Abstract: Dengue fever is a vector-borne infectious disease, which is known to quickly develop and spread under favorable weather conditions. This presence of the disease is also affected by societal behaviors (population migration and prevention attitude towards the disease). We apply a spatial and temporal extension of the kernel density estimation algorithm to map space-time clusters of dengue fever in Cali, Colombia for the year of 2010. We conduct the Space-Time Kernel Density Estimation (STKDE) in a parallel computational framework to account for the computational complexity involved. We extract intricate disease dynamics in an interactive manner, using a powerful 3D environment. Computational and cartographic impacts of varying space-time bandwidths are presented. The findings from our work can help better understand the dynamics of a quickly spreading disease.

Keywords: dengue fever, kernel density estimation, parallel computing, space-time visualization

1. Introduction

The outbreak and communicability of infectious diseases across the world are driven by an array of complex interrelated factors and processes, such as rapid urbanization, human mobility, changes in public health policy, and global climate change (Cooley et al. 2008; Eastin et al. 2014; Hu et al. 2012; Kanobana et al. 2013, Wu et al. 2009). Infectious diseases such as malaria or dengue fever, pose a critical threat to vulnerable human populations such that timely responses are necessary to reduce the burden caused by the diseases. Dengue fever for instance is known to vary through time and space, due to a number of factors including human host, virus, mosquito acting as disease-vector and environment (Mammen et al. 2008). To implement appropriate control measures, public health organizations and policy makers must rely on accurate and timely predictions of disease foci monitoring and analyzing them under critical space-time conditions. A better understanding on the space-time signature of infectious diseases such as their rate of transmission and tendency to cluster should help epidemiologists and public health officials better allocate prevention measures.

Geographical Information Systems (GIS) and associated spatial analysis methods (Haining 1990; Goodchild et al. 1992; Anselin 1999; Fischer and Getis 2009) have received considerable attention in the field of spatial epidemiology (Cromley and McLafferty 2011). GIS can effectively organize individual or aggregated data, and map the magnitude and expansion of these diseases over time. Ultimately, results from GIS and spatial analysis have the potential to reduce disease burden by generating new information for the public and health agencies, leading to improvement on development of preventive measures and strategic allocation of control resources.

In spatial epidemiology, the development of computational techniques for the identification and the visualization of space-time clusters in large databases is a challenge (Delmelle, Kim, et al. 2013, Goovaerts and Goovaerts, this issue, Delmelle et al. 2014). Our chapter contributes to the field of space-time clustering, specifically the use of Space-Time

Kernel Density Estimation (STKDE) for infectious diseases and the visualization of disease dynamics in a 3D environment. The results provide a sense of where outbreaks of dengue fever linger around for a longer time (persistence). These patterns might generate clues on why dengue outbreaks tend to remain around particular areas. Together with information and expertise from local authorities, intervention programs may be conducted about to address particular (unique) settings.

The chapter is organized as follows: Section 2 discusses the importance of spatial and space-time analytical methods, and existing visualization frameworks for epidemiology. Section 3 discusses the contribution of visual analytics for space-time data and introduces the extension of the Kernel Density Estimation (KDE) in time (STKDE). STKDE is particularly demanding, from a computational perspective, and to address this issue, we integrate STKDE with a parallel computing environment, in Section 4. We illustrate our approach on a set of dengue fever cases in the city of Cali, Colombia (2010). A static 3D visualization is used to illustrate the spatio-temporal characteristics of this infectious disease. Directions for future research are presented in the last section.

2. Space-time visual analytics

Representing the multi-dimensionality of geographical space and its phenomena is a complex task. Over time, cartographers have proposed a wide variety of techniques; mostly two-dimensional, static maps (Bertin, 1983). In spatial epidemiology, disease maps are generally presented in one of two forms (Cromley and McLafferty 2011): at an aggregated level, divided by the population at risk, resulting in a choropleth map, or at the individual level as a scatter map. As scatter maps become very cluttered when incorporating a large number of events, an alternative consists of producing a kernel distribution map that generates a smooth probability raster that facilitates the discovery of clusters (Bailey and Gatrell 1995).

As part of the multi-dimensionality of spatial data, temporal coordinates are often present, for instance the time stamp associated with a particular event. Since the development of the space-time cube concept (Hägerstrand 1970), several analytical and visualization strategies have been developed to integrate the temporal dimension in spatial analysis (Kwan 2004; Miller 2005; Jacquez, Greiling, and Kaufmann 2005). The availability of personal computers, advances in Geographical Information Systems technology, and increasingly efficient graphic processing power (Peterson 1995) has allowed the development of new tools and techniques to integrate the temporal dimension in the form of cartographic movies (Tobler 1970), animations in two and three dimensions (Moellering 1980; Harrower and Fabrikant 2006; Brunson, Corcoran, and Higgs 2007) and interactive maps or geo-browsers (Harrower 2004; Dykes, MacEachren, and Kraak 2005; Hruby, Miranda, and Riedl 2009). Graphic user interfaces have been tailored to address particular needs (Jacquez, Greiling, and Kaufmann 2005; Rogerson and Yamada 2008; Delmelle et al. 2011). The latter techniques are particularly well-suited to analyze infectious diseases exhibiting cyclic patterns—outbreaks can surge and resurface at particular space-time locations. Thakur and Hanson (2010) developed a pictorial representation based on the space-time cube framework, providing, in a single display, an overview and details of a large number of time-varying information. Their approach is discrete using aggregated county data.

In this chapter, we follow the continuous approach set forth by Andrienko et al. (2010) and Demšar and Virrantaus (2010) by extending the space-time prism framework to monitor and visualize disease dynamics. Recently, Fang and Lu (2011) proposed a 3D space-time cube, which integrates air pollution scenarios. The base of this cube describes the spatial variation of air pollution across a traditional 2D space while the height is used as the temporal dimension. As time progresses, the change of air pollution for each location within the base 2D space is continuously updated. Time periods are represented as layers, which are separated from each other by an offset. However, 3D layers may form cluttered maps, even with a small number of layers.

In certain cases, animations may work better than three-dimensional mapping and lead to a more accurate detection of space-time clusters. However, several variables prevent full control over these animations, as, among others, frame duration and speed of transition must be calibrated (Harrower and Fabrikant 2008). In spite of the advances, 3D visualization remains a cartographic challenge (Langran, 1994), and not enough is known about its effectiveness for mapping the temporal dimension along the third axis (Fabrikant 2005; Andrienko et al. 2010). In this chapter, we use a 3D space-time cube framework to map the stability and strength of spatial clusters over time.

3. Methodology

a. Kernel Density Estimation (KDE)

Kernel Density Estimation (KDE) (Bailey and Gatrell 1995; Delmelle 2009) is a spatial analytical technique, which maps the spatial distribution of point events across an area. KDE produces a raster surface reflecting the spatial variation of the probability that an event will occur. One of the benefits of KDE is its ability to delimit the spatial extent of disease occurrences (Delmelle et al. 2011). For infectious diseases, these maps are used in conjunction with prevention and control programs to guide disease-vector control and/or surveillance activities (Eisen and Eisen 2011; Eisen and Lozano-Fuentes 2009). KDE is computed at each grid cell, which receives a higher weight if it has a larger number of observations in its surrounding. Let $s(x,y)$ represents a location in an area R where the kernel density estimation needs to be estimated, and s_1, \dots, s_n the locations of n observed events (Silverman 1986):

$$\hat{f}(x, y) = \frac{1}{nh_s^2} \sum_i I(d_i < h_s) k_s\left(\frac{x-x_i}{h_s}, \frac{y-y_i}{h_s}\right) \quad (1)$$

The term h_s is the search radius, or spatial bandwidth, which governs the amount of smoothing, and k_s is a standardized weighting function, known as the kernel that determines

the shape of the weighting function. Here d_i is the distance between location s and event s_i , which is constrained by $d_i < h_s$, such that only the points which fall within the chosen bandwidth contribute to the estimation of the kernel density at s . The number of points participating in the kernel density estimation affects the computation time linearly, while smaller cell sizes (finer grid) result in an exponential increase in the overall computation time.

Point events generally have a time stamp associated with them $s(x,y,t)$. One critical challenge is time integration in KDE, which may help to address the questions of (1) whether the distribution of events varies over time, and (2) whether the occurrence of the underlying process is repeated in certain areas and exhibit a cyclical pattern, in turn indicating a spatio-temporal process. Two approaches exist to integrate the temporal dimension in the KDE. In the first approach, we query data for different temporal intervals -time period 1, time period 2...time period t-, and the spatial kernel density is repeated sequentially for those intervals. We call this approach sequential KDE –sKDE-. Usually, the resulting kernel density images are arranged in an animation framework or side-by-side as a multiple. In the second approach, the kernel density estimation method is explicitly extended in time –STKDE- by adding a temporal bandwidth (Nakaya and Yano 2010; Demšar and Virrantaus 2010), and visualized in a 3D environment. Computationally, the space-time kernel density estimation (STKDE) is much more challenging and cartographically more complex, but it has the advantage of summarizing the spatio-temporal clustering pattern in one image. The two approaches are explained in detail in the following paragraphs.

In the Sequential Kernel Density Estimation (sKDE) the KDE procedure can be repeated over several time intervals (granularity of one day, one week, one month), producing different KDE layers. These layers are then arranged in a mosaic framework side-by-side. This so-called “multiple” arrangement has the disadvantage that users must move from one image to another and reconstruct the movement of the clusters. An alternative proposed earlier is the use of animation (Dorling 1992; Harrower and Fabrikant 2006; Brunsdon,

Corcoran, and Higgs 2007). The sequential Kernel Density Estimation does not explicitly take time into account; rather, each map is a snapshot of a particular situation at a specific time interval.

According to Nakaya and Yano (2010) and Demšar and Virrantaus (2010), a mosaic of two dimensional kernel densities does not facilitate simultaneous visualization of the geographical extent and duration of point patterns and spatial clusters, unless they are adequately arranged in an animation framework, or stacked on top of each other in a 3D environment. An alternative is the extension of the kernel density estimation in time (STKDE). The STKDE approach requires mapping a volume of probabilities. Its main advantage lies in seeing all probabilities and clusters at once, rather than the need to recreate a mental image through animation. We apply an extension of Silverman's spatial kernel density which incorporates the temporal dimension, as described in Nakaya and Yano (2010). The space-time density $\hat{f}(x, y, t)$ at s is thus estimated by:

$$\hat{f}(x, y, t) = \frac{1}{nh_s^2 h_t} \sum_i I(d_i < h_s, t_i < h_t) k_s \left(\frac{x-x_i}{h_s}, \frac{y-y_i}{h_s} \right) k_t \left(\frac{t-t_i}{h_t} \right), \quad (2)$$

where d_i and t_i are the Euclidean (or network) distance and temporal differences between location s and event s_i . $I(d_i < h_s, t_i < h_t)k_s$ is an indicator function taking value 1 if $d_i < h_s$ and $t_i < h_t$. h_s is the search radius (or bandwidth), governing the amount of smoothing. h_t is the temporal search window. k_s is a standardized weighting function, known as the kernel that determines the shape of the weighting function. k_t is a standardized temporal weighting function. Generally, a space-time count statistic (K-function) can be used to estimate the optimal global bandwidths ($h_s^2 h_t$) in space and time, although different approaches have been suggested.

b. STKDE implementation

We used the procedure presented in Figure 1 to compute the STKDE. First, based on the extent of the study region and a desired voxel¹ size, a 3D grid is generated. This process is also known as three-dimensional discretization. Second, for each voxel centroid, we compute the space-time kernel density (z_0) using appropriate bandwidths (h_s, h_t)² and Equation 2 to identify the disease events that will participate in the computation. An additional constraint is added that only considers nearby points. Voxels that fall outside of the study region or where the density value is equal to zero ($z_0=0$) are excluded. Both added constraints reduce computational time. The STKDE algorithm is coded in the Python environment. Finally, density results are visualized in a three-dimensional visualization environment (Voxler, Golden, CO) where the appearance of the cluster can be adjusted according to the distribution of density values. To detect micro-patterns, a fine grid is generally preferred to the cost of a heavier computation and longer rendering time. Results are visualized in a 3D environment, allowing a better understanding of complex disease dynamics in an interactive manner.

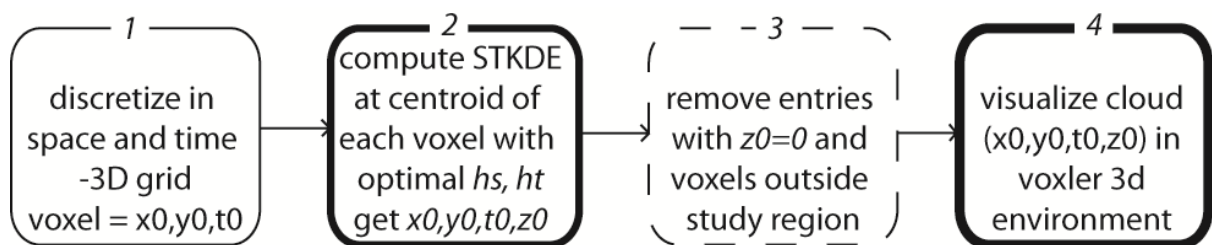


Figure 1. STKDE computing framework. Boxes in bold (2) and (4) denote computing intensive procedures, while the dashed box (3) is optional.

c. A parallel computing approach

The estimation of space-time kernel densities in point pattern data consumes considerable amount of computing resources. This method requires handling each voxel in the space-time cube at a time. Consequently, when the number of voxels or the number of points in the

1 A voxel can be conceived as the extension of a grid cell in a third dimension. It is a volumetric element.

2 A space-time K-function is used to estimate the optimal bandwidths of space-time clusters of dengue fever (Delmelle et al. 2011).

spatiotemporal point pattern is excessively large, a significant amount of computation may be required to complete the derivation of space-time kernel densities. Thus, we prefer using a parallel computing approach (Armstrong 2000; Wang and Armstrong 2009; Tang and Bennett 2011; Tang 2013) to cope with the intense computational efforts related to the derivation of spatiotemporal kernel density. In this study, we follow the strategy proposed by Wilkinson and Allen (2004) for the efficient estimation of space-time kernel densities. The parallel computing resources that we used include 54 nodes with 432 computing cores. A dual Intel Xeon X5570 processor with 2.93 GHz of clock rate was used, with each processor having 24 GB of memory.

4. Results

a. Dengue fever and geospatial datasets

Dengue fever, which is an arboviral disease endemic to tropical and subtropical areas is among the most dangerous infectious diseases. It has a global presence and poses a threat to more than 2.5 million people. Dengue fever is a problem to communities and health entities, necessitating the control and the prevention of the virus (Méndez et al. 2006; WHO 2009). Dengue fever is transmitted to humans by a mosquito of the genus *Aedes* (Monath 1988). The *Aedes aegypti* mosquito lives and reproduces in warm climates where temperatures range between 18^o and 25^o C (Wu et al. 2009).

Colombia is one of the many countries where dengue fever is endemic and constitutes a serious health problem. The population living in areas at risk of contracting the disease totals 26 million individuals. These areas are characterized by elevations below 1,800 meters (Colombianos 2011). The City of Cali, which is the focus of this study, is considered an endemic dengue fever zone. It is located in the valley of the Cauca River 1,000 meters above sea level and has an average daily temperature of 23^oC. Annual precipitation in the driest

zones reaches 900 mm and 1,800 mm in the rainiest. The city's annual precipitation average is 1000 mm (Cali 2008). According to the health municipality of the City of Cali (Cali 2010) there have been three severe dengue outbreaks between 1990 and 2009: 1995, 2002, and 2005 (Cali 2010). During 2009 and the first quarter of 2010 more than 7,000 cases of dengue fever were reported in the city (Cali 2010). By the end of January of that year a total of 990 dengue fever cases were registered with the number increasing to 3,540 by week 10 (mid-March). At this point the signs of an epidemic were evident. By August of 2010 a total of 9,310 cases of dengue fever had been reported. In this chapter, we map space-time clusters of individuals infected by dengue fever within the city of Cali for the year 2010, a year that corresponds to a strong outbreak of the disease.

The dengue fever dataset corresponds to cases of dengue reported in the “Sistema de Vigilancia en Salud Pública” (SIVIGILA, English: Public health surveillance system) for the City of Cali (provided by the health municipality of the City of Cali) for the year 2010. An entire description of the geospatial dataset, and geocoding procedure is given in (Delmelle, Casas, et al. 2013). Individuals report dengue fever symptoms on a daily basis (unit=Julian date) at a local hospital. Hospital records include patient information (sex, age, race, address, neighborhood, and occupation), date of diagnosis, epidemiological week, and day symptoms started. There were 11,760 cases reported in 2010. The data was geocoded to the intersection level to guarantee patient privacy (Kwan, Casas, and Schmitz 2004). Eighty one percent of the total cases were perfectly matched. The 19% that could not be matched constitute non-existent addresses or addresses with errors that could not be fixed. From the 9,555 that were successfully geocoded, as described in (Delmelle, Casas, et al. 2013), the majority of the cases occurred during the first 4-5 months of the year, after which the municipality invested time and efforts to further eradicate mosquito breeding habitats.

We now illustrate the results from the STKDE algorithm on all patients exhibiting symptoms of dengue fever in Cali, Colombia, in 2010. We discuss the benefits of the parallel approach, and the sensitivity of the STKDE.

b. Parallel computing results

We use a space-time K-function, a scan statistic (see HELP in Delmelle et al. (2011)), to identify the geographical and temporal scale at which clusters of dengue are the strongest (determined as $h_s=1500\text{m}$ and $h_t=10\text{days}$). We implement the STKDE algorithm with those space-time parameters. We also estimate the robustness and sensitivity of the STKDE algorithm against different cell sizes and bandwidths, among others.

Figure 2a reports the running time to conduct the STKDE for the entire city of Cali on a single CPU, and hereafter referred to as ‘sequential’. The STKDE is estimated on a 3D grid of resolution $100\text{m} * 100\text{m} * 1\text{ day}$. The running time significantly decreases when using larger voxel sizes, since STKDE is estimated on a much smaller set of 3D gridded data points. The same reduction in running time is observed in Figure 2b which summarizes the maximum computational effort when using a parallel computing approach. Although the shapes of the curves in Figure 2a and Figure 2b are similar, the time range is much smaller in the latter. As the cell size increases, the running time to compute the STKDE decreases, in an exponential fashion. Figure 3a reports the ‘sequential’ time for different spatial bandwidths. As expected, the running time increases in a linear fashion when using larger bandwidths, since a greater number of points are included in the computation. The same pattern is observed in Figure 3b, which illustrates the maximum computational effort when using a parallel computing approach.

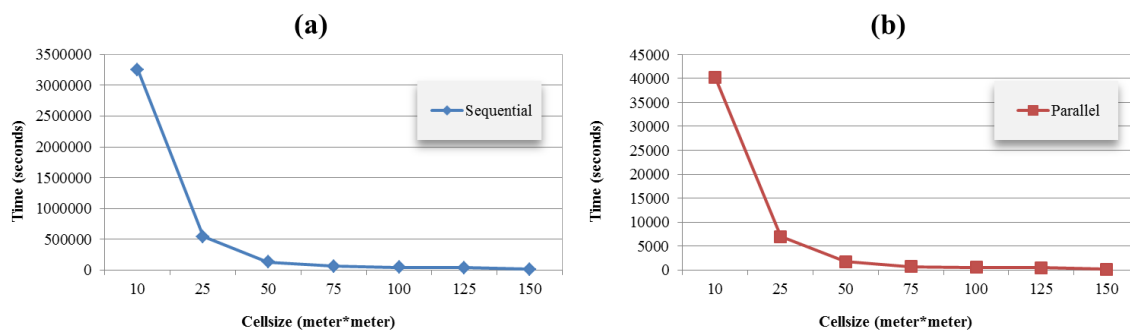


Figure 2. Running time for the STKDE on one CPU (a), 96 CPUs(b), speedup (c) and sensitivity to search radius in (d) based on different cell sizes. Note the values along the Y-axis are different.

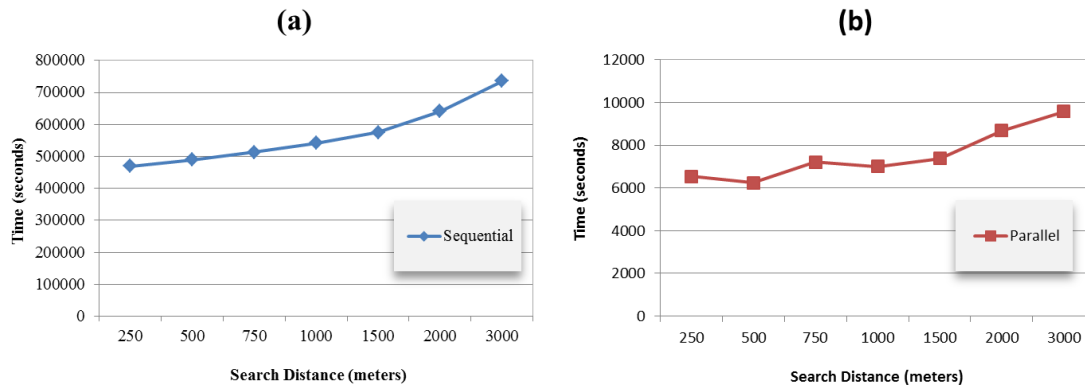


Figure 3. Sensitivity of the STKDE running with variation in spatial bandwidth, on one CPU (a), 96 CPUs(b). Note the values along the Y-axis are different.

c. 3D visualization

The kernel density volume is extracted by computing the Kernel Density Estimation of each voxel in our 3D area. It is then visualized by color-coding each voxel according to its kernel density value. The transparency level is also adjusted to concentrate the focus on those regions with higher density values (Figure 4). The KDE values range from 0 to 1 (on the map). Voxels having a KDE of 0.3 or less are colored in dark and lighter blue shades and voxels with a value between 0.3 and 0.5 are colored yellow. Voxels between 0.5 and 0.7 are colored green and voxels with higher KDE values are colored in red or purple tones. The highest KDE values are usually found in a couple of cores within the voxel cloud (not at the edges). Since those higher densities are the phenomenon we are interested to capture and thus visualize, different transparency levels are used depending on the KDE value of each voxel. In this case, voxels with lower KDE value (<0.25) were brought to a high transparency level, allowing the visualization of underlying voxels, with higher KDE values. For values of 0.3 to 1 the transparency was lowered in a linear fashion.

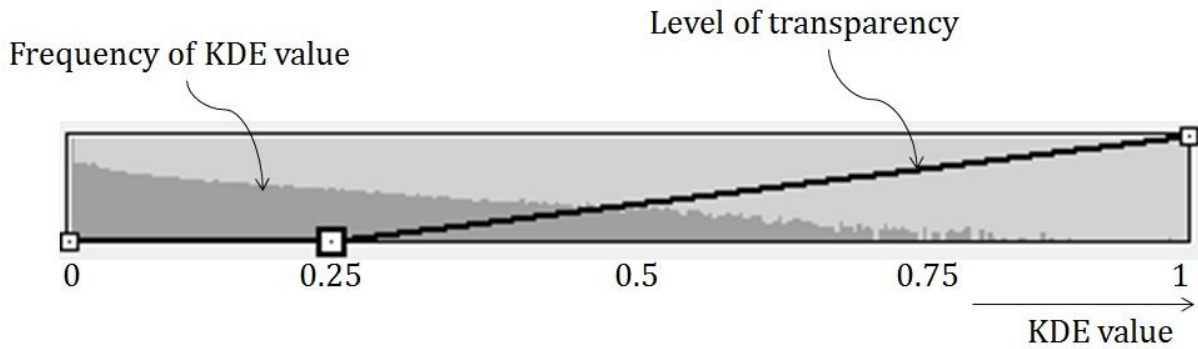


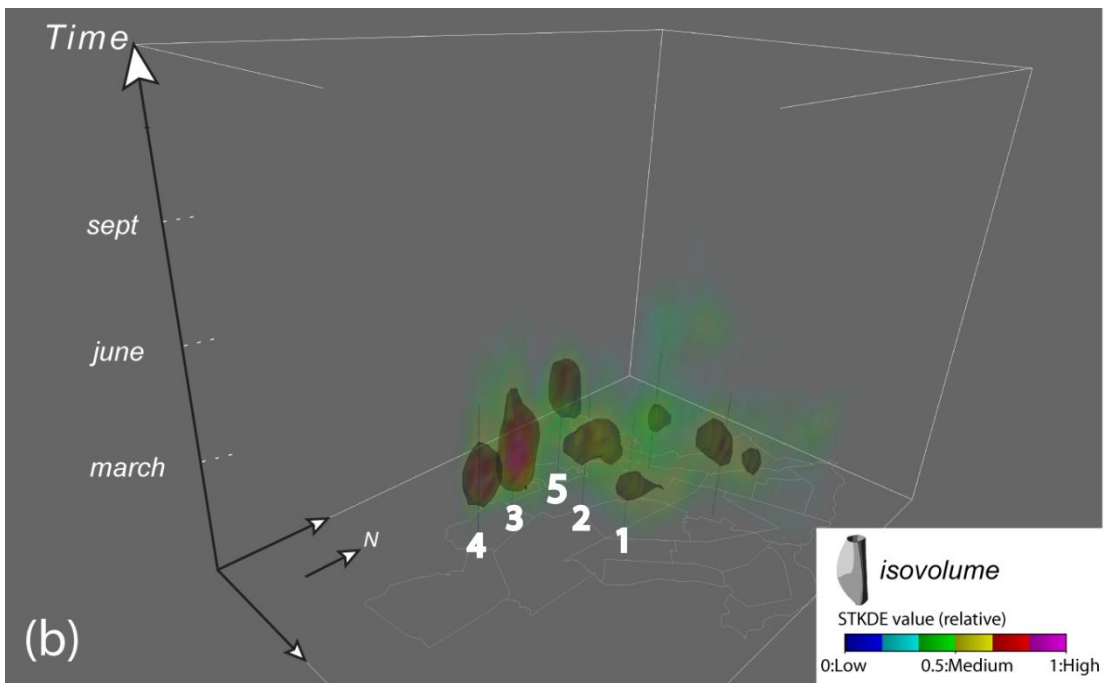
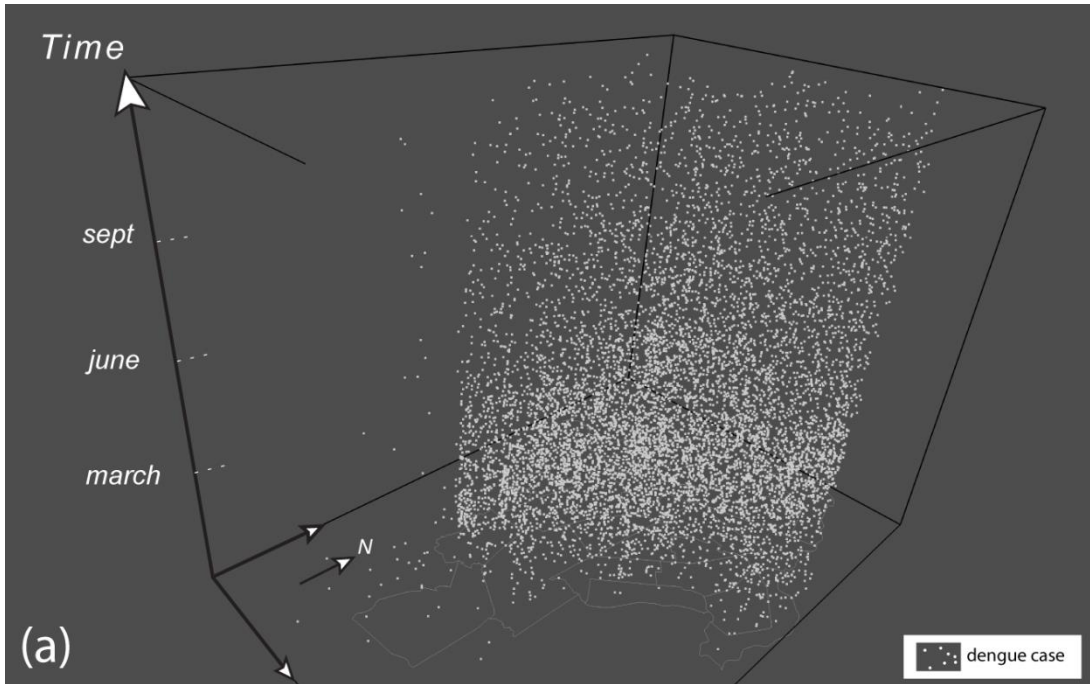
Figure 4. Transparency scheme adopted in Voxler for visualizing STKDE values ranging from 0 to 1 (on the map).

We reinforce the importance of clusters by using so-called ‘egg shells’. These are created by computing an isosurface around voxels having a value of 0.7. When visualizing these isosurfaces, interestingly they create an envelope capturing areas with higher KDE values. Also, these isosurfaces allow us to visualize the shape of the outbreak in space and time. This isosurface can be visualized in two ways, one is a smooth surface, and the other one is a TIN-like surface. Both surface types have the same shape and encapsulate the same space-time areas, but are represented in a different way.

d. 3D visualization results

We map the space-time stamp of dengue cases in Figure 5a and the space-time kernel density in Figures 5b with isovolumes and 5c with triangulated irregular networks using $h_s=1500\text{m}$ and $h_t=10\text{days}$ at a discretization level of $125\text{m} \times 125\text{m} \times 1\text{ day}$ (finer discretization level may provide more details, but at a cost of a larger storage). The distribution of cases is particularly strong in the beginning of the year. In Figures 5b and 5c, the observed pattern clearly shows cyclic reoccurrence of the cluster of the disease, although this particular infectious disease may follow a pyramid like-pattern: dengue fever may saturate in the population over time and as a consequence exhibits skinnier clusters. Several space-time clusters are constant, with high intensity. These correspond to areas in the central part of the city (clusters 1 and 2), the west side close to the foothills (cluster 5), while clusters (3) and (4) are in proximity in the

south west part of the city (see Figure 5b). All clusters are more intense in the beginning of the year since the highest number of cases occurred between January and March of 2010. Among the five clusters, clusters (1) and (2) cover a larger spatial extent, but short in time. Cluster (1) is concentrated throughout a relatively shorter time period compared to the other four clusters. This is an area with old urban neighborhoods composed of households with large families, which increases the risk of people being exposed to the disease. On the other hand, policy measures might work more effectively in those areas because of the pre-existing bond between people and their willingness to work together to eradicate the epidemic, which might be the reason for the quick eradication of the disease in that area. Cluster (5) has a more focused spatial extent in the foothills to the west of the city. It corresponds to a neighborhood of low stratification where individuals are more likely to maintain water containers serving as breeding sites for the mosquito to reproduce. This cluster prevails over time, more so than cluster (1) and (2). Clusters (3) and (4) are located in Commune 18 (a commune is a group of neighborhoods). This commune is characterized by the presence of a military base with a high concentration of individuals living and interacting in very close proximity due to the confined space. Mosquitoes usually do not fly further than 200 meters. However, in parts of the city where higher densities are encountered, one mosquito holding the virus might cause a large amount of people being infected. This explains the shape of the cluster, small extent and long period of time. This particular commune has been identified by the secretary of health municipality of the city of Cali as being at high risk of contracting dengue fever.



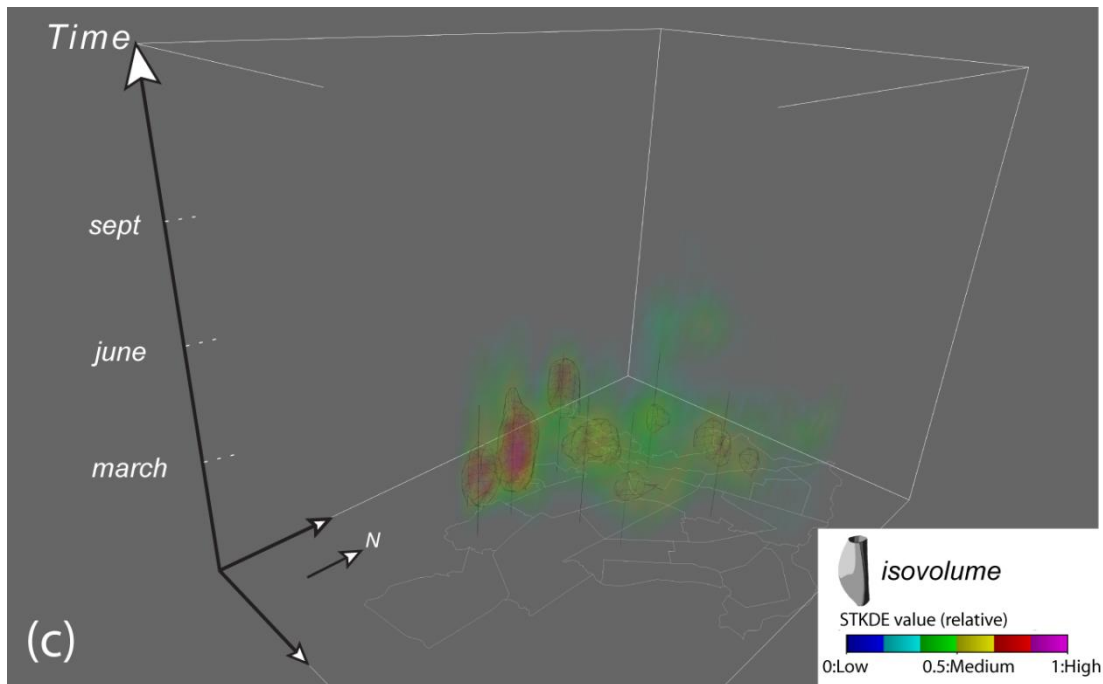


Figure 5. Space-time distribution of dengue fever cases for the year 2010 in Cali, Colombia in (a). STKDE using a cell size of 125 meters with shaded isovolumes in (b) and isovolumes in a triangulated fashion in (c). Clusters numbers (1)-(5) are discussed in the text.

5. Discussion and future research

Dengue fever is a vector-borne infectious disease, which can take dramatic proportions when conditions (e.g. population, disease-vector, climate, behavior) are optimal. Mobility of humans is known to affect the spread of the disease. However, less research has been conducted on visualizing clusters of infectious diseases, in particular, in a spatiotemporal dimension. In this chapter, we apply a spatial and temporal extension of the kernel density estimation algorithm to map space-time clusters of dengue fever in Cali, Colombia for the year of 2010. We used a parallelized computation framework which, significantly reduces the running time and thus allows the problem solving to be more manageable. We illustrate and extract complex disease clusters using a 3D environment. We can observe different cluster shapes, which might correspond to different neighborhood and population setting. Elongated temporal clusters denote that the disease tend to remain contained over a geographic area for a longer time (for instance, a military base that tend to be hermetic, meaning the disease does not spread further form the base borders). Larger yet less intense

clusters which are less intense generally occur in areas with a high degree of human movement. Such visualizations are very valuable to better understand the resurgence cycle of infectious diseases and necessary for public health managers to decide on the allocation of appropriate resources. The findings from our work can help better understand the dynamics of a quickly spreading disease and may help build different strategies depending on distinct socio-environmental settings within the area at stake.

We see the followings for future research. First, the extension of the kernel density estimation in time can be used to estimate the speed at which the disease tend to spread, and whether it tends to have a directional preference. Second, computational time could further be reduced by using space-time adaptive (and directional) windows. Third, it is necessary to simulate points datasets (Monte Carlo simulations) to extract the significance of the clusters. Of importance is the accuracy of the geocoded data itself (Delmelle et al. 2014, DeLuca and Kanaroglou, this issue): if the accuracy is very low, authorities might want to improve their surveillance strategies in the future. Finally, more research is needed to evaluate the effectiveness of 3D versus animated cartography when mapping disease cluster dynamics.

Authors biography

Dr. Eric Delmelle and Dr. Wenwu Tang are assistant professors in the Geography and Earth Sciences Department at the University of North Carolina at Charlotte. Dr. Delmelle's interests are in the development of spatial modeling techniques to the field of spatial epidemiology/optimization. Dr Tang's research interests are in the domain of Agent-Based Models and Spatio-Temporal Simulation, high-performance and parallel computing as well as GIS & Spatial Analysis and Modeling. Meijuan Jia and Coline Dony are graduate students in Geography at the University of North Carolina at Charlotte. Dr. Irene Casas is an associate professor in the department of Social Sciences at Louisiana Tech and has conducted research in Cali, Colombia with spatial epidemiologists to better understand health care provision and access.

References

- Andrienko, G., N. Andrienko, U. Demsar, D. Dransch, J. Dykes, S. I. Fabrikant, M. Jern, M.-J. Kraak, H. Schumann, and C. Tominski. 2010. Space, time and visual analytics. *International Journal of Geographical Information Science* 24 (10):1577-1600.
- Anselin, L. 1999. Interactive techniques and exploratory spatial data analysis. In *Geographical Information Systems*, eds. P. Longley, M. Goodchild, D. Maguire and D. Rhind. New York: Wiley.
- Armstrong, M. P. 2000. Geography and computational science. *Annals of the Association of American Geographers* 90 (1):146-156.
- Bailey, T., and Q. Gatrell. 1995. *Interactive Spatial Data Analysis*. Edinburgh Gate, England: Pearson Education Limited.
- Brunsdon, C., J. Corcoran, and G. Higgs. 2007. Visualizing space and time in crime patterns: A comparison of methods. *Computers, Environment and Urban Systems* 31:52-75.
- Cali, A. d. S. d. 2008. Cali en cifras. Cali: Alcaldia de Cali.
- Cali, S. d. S. P. M. d. 2010. *Historia del dengue en Cali. Endemia o una continua epidemia*. Cali: Secretaria de Salud Publica Municipal de Cali.
- Colombianos, M. G. *Guia de atención al dengue* 2011 [cited].
- Cooley, P., L. Ganapathi, G. Ghneim, S. Holmberg, W. Wheaton, and C. R. Hollingsworth. 2008. Using influenza-like illness data to reconstruct an influenza outbreak. *Mathematical and computer modelling* 48 (5):929-939.
- Cromley, E., and S. McLafferty. 2011. *GIS and Public Health*. New York: Guilford Press.
- Delmelle, E. 2009. Point Pattern Analysis. In *International Encyclopedia of Human Geography*, eds. R. Kitchin and N. Thrift, 204-211. Oxford: Elsevier.
- Delmelle, E., I. Casas, J. Rojas, and A. Varelo. 2013. Modeling Spatio-Temporal Patterns of Dengue Fever in Cali, Colombia. *International Journal of Applied Geospatial Research*.
- Delmelle, E., E. Delmelle, I. Casas, and T. Barto. 2011. H.E.L.P: a GIS-based health exploratory analysis tool for practitioners. *Applied Spatial Analysis and Policy* 4 (2):113-137.
- Delmelle, E., C. Kim, N. Xiao, and W. Chen. 2013. Methods for space-time analysis and modeling: An overview. *International Journal of Applied Geospatial Research*.
- Delmelle, E., Dony, C., Casas, I., Jia, M., & Tang, W. (2014). Visualizing the impact of space-time uncertainties on dengue fever patterns. *International Journal of Geographical Information Science*, (ahead-of-print), 1-21.
- Deluca P. and P. Kanaroglou (this issue). An Assessment of Online Geocoding Services for Health Research in a Mid-Sized Canadian City.
- Demšar, U., and K. Verrantaus. 2010. Space-time density of trajectories: exploring spatio-temporal patterns in movement data. *International Journal of Geographical Information Science* 24 (10):1527-1542.
- Dorling, D. 1992. Stretching space and splicing time: From cartographic animation to interactive visualisation. *Cartography and Geographic Information Systems* 19:215-227.
- Dykes, J., A. M. MacEachren, and M.-J. Kraak. 2005. *Exploring geovisualization*: Pergamon.
- Eastin M., Delmelle E.M, Casas I, Wexler J. and C. Self. (2014). Comparison of intra- and inter-seasonal auto-regressive modeling for predicting Dengue outbreaks in a tropical environment of Colombia. *American Journal of Tropical Medicine and Hygiene*.

- Eisen, L., and R. Eisen. 2011. Using geographic information systems and decision support systems for the prediction, prevention, and control of vector-borne diseases. *Annual Review of Entomology* 56 (1):41-61.
- Eisen, L., and S. Lozano-Fuentes. 2009. Use of mapping and spatial and space-time modeling approaches in operational control of aedes aegypti and dengue. *PLoS Negl Trop Dis* 3 (4):e411.
- Fabrikant, S. I. 2005. Towards an understanding of geovisualization with dynamic displays: Issues and prospects. Paper read at Proceedings, American Association for Artificial Intelligence (AAAI) 2005 Spring Symposium.
- Fang, T. B., and Y. Lu. 2011. Constructing a Near Real-time Space-time Cube to Depict Urban Ambient Air Pollution Scenario. *Transactions in GIS* 15 (5):635-649.
- Fischer, M., and A. Getis. 2009. *Handbook of Applied Spatial Analysis: Software Tools, Methods and Applications*.
- Goodchild, M. F., R. Haining, S. Wise, G. Arbia, L. Anselin, E. Bossard, C. Brunson, P. Diggle, R. Flowerdew, M. Green, D. Griffith, L. Hepple, T. Krug, R. Martin, and S. Openshaw. 1992. Integrating GIS and spatial data analysis - Problems and possibilities. *International Journal of Geographical Information Systems* 6 (5):407-423.
- Goovaerts P. and M. Goovaerts (this issue). Space-time analysis of late-stage breast cancer incidence in Michigan.
- Hägerstrand, T. 1970. What about people in regional science? *Papers in regional science* 24 (1):7-24.
- Haining, R. 1990. *Spatial Data Analysis in the Social and Environmental Sciences*. Cambridge: Cambridge University Press.
- Harrower, M. 2004. A look at the history and future of animated maps. *Cartographica: The International Journal for Geographic Information and Geovisualization* 39 (3):33-42.
- Harrower, M., and S. Fabrikant. 2006. The role of map animation for geographic visualization. In *Geographic Visualization: Concepts, Tools and Applications*, eds. M. Dodge, M. McDerby and M. Turner: Wiley.
- Harrower, M., and S. Fabrikant. 2008. The role of map animation for geographic visualization. *Geographic visualization*:49-65.
- Hruby, F., R. Miranda, and A. Riedl. 2009. Bad Globes & Better Globes—multilingual categorization of cartographic concepts exemplified by “map” and “globe” in English, German and Spanish. Paper read at Proceedings of the 24th International Cartography Conference (ICC 2009), Santiago, Chile 2009.
- Hu, W., A. Clements, G. Williams, S. Tong, and K. Mengersen. 2012. Spatial patterns and socioecological drivers of dengue fever transmission in Queensland, Australia. *Environmental health perspectives* 120 (2):260.
- Jacquez, G., D. Greiling, and A. Kaufmann. 2005. Design and implementation of a space-time intelligence system for disease surveillance. *Journal of Geographical Systems* 7 (1):7-23.
- Kanobana, K., B. Devleeschauwer, K. Polman, and N. Speybroeck. 2013. An agent-based model of exposure to human toxocariasis: a multi-country validation. *Parasitology*:1-13.
- Kwan, M.-P. 2004. GIS methods in time-geographic research: Geocomputation and geovisualization of human activity patterns. *Geografiska Annaler B* 86:205-218.
- Kwan, M.-P., I. Casas, and B. C. Schmitz. 2004. Protection of geoprivacy and accuracy of spatial information: how effective are geographical masks? *Cartographica* 39 (2):15-28.
- Mammen, M. P., C. Pimgate, C. J. M. Koenraadt, A. L. Rothman, J. Aldstadt, A. Nisalak, R. G. Jarman, J. W. Jones, A. Srikiatkachorn, C. A. Ypil-Butac, A. Getis, S.

- Thammapalo, A. C. Morrison, D. H. Libraty, S. Green, and T. W. Scott. 2008. Spatial and temporal clustering of dengue virus transmission in Thai villages. *PLoS Medicine* 5:1605-1616.
- Méndez, F., M. Barreto, J. F. Arias, G. Rengifo, J. Muñoz, M. E. Burbano, and B. Parra. 2006. Human and mosquito infections by dengue viruses during and after epidemics in a dengue-endemic region of Colombia. *The American Journal of Tropical Medicine and Hygiene* 74:678-683.
- Miller, H. 2005. A measurement theory for time geography. *Geographical Analysis* 37:17-45.
- Moellering, H. 1980. The real-time animation of three-dimensional maps. *The American Cartographer* 7 (1):67-75.
- Monath, T. ed. 1988. *The arboviruses: epidemiology and ecology*. Boca Raton, FL: CRC Press.
- Nakaya, T., and K. Yano. 2010. Visualising crime clusters in a space-time cube: an exploratory data-analysis approach using space-time kernel density estimation and scan statistics. *Transactions in GIS* 14 (3):223-239.
- Peterson, M. P. 1995. Interactive and animated cartography.
- Rogerson, P., and I. Yamada. 2008. *Statistical Detection and Surveillance of Geographic Clusters*. Boca Raton, Florida: CRC Press.
- Silverman, B. W. 1986. *Density Estimation for Statistics and Data Analysis*. London: Chapman and Hall.
- Tang, W. 2013. Parallel construction of large circular cartograms using graphics processing units. *International Journal of Geographical Information Science* (ahead-of-print):1-25.
- Tang, W., and D. A. Bennett. 2011. Parallel agent-based modeling of spatial opinion diffusion accelerated using graphics processing units. *Ecological Modelling* 222:3605-3615.
- Thakur, S., & Hanson, A. J. (2010). A 3D visualization of multiple time series on maps. In *Information Visualisation (IV), 2010 14th International Conference* (pp. 336-343). IEEE
- Tobler, W. R. 1970. A computer movie simulating urban growth in the Detroit region. *Economic geography* 46:234-240.
- Wang, S., and M. P. Armstrong. 2009. A theoretical approach to the use of cyberinfrastructure in geographical analysis. *International Journal of Geographical Information Science* 23 (2):169-193.
- WHO. 2011. *Dengue and dengue haemorrhagic fever - Fact sheet no. 117*. WHO 2009 [cited January, 17, 2011 2011]. Available from <http://www.who.int/mediacentre/factsheets/fs117/en/>.
- Wu, P.-C., J.-G. Lay, H.-R. Guo, C.-Y. Lin, S.-C. Lung, and H.-J. Su. 2009. Higher temperature and urbanization affect the spatial patterns of dengue fever transmission in subtropical Taiwan. *The Science of the Total Environment* 407:2224-2233.